Top Organomet Chem (2006) 17: 57–82
DOI 10.1007/3418_003

Published online: 12 April 2006

Catalytic Nickel–Iron–Sulfur Clusters: From Minerals to Enzymes

Anne Volbeda · Juan C. Fontecilla-Camps (✉)

Laboratoire de Cristallographie et de Cristallogenèse des Protéines,
Institut de Biologie Structurale J.P. Ebel (CEA-CNRS-UJF), 41 rue Jules Horowitz,
38027 Grenoble Cédex 1, France
juan.fontecilla@ibs.fr

Abstract The geochemical theory of the origin of life proposes that primordial, pre-biotic reactions were carried out in a metal-sulfide-rich environment similar to that found near hot springs at the ocean floor. Many contemporary experiments have shown that reactions reminiscent of those carried by extant anaerobic microorganisms involving gases such as CO, CO_2 and H_2, can indeed take place abiotically in the presence of iron and nickel sulfides. Here we discuss some of these reactions and compare them to those catalyzed by NiFeS-containing enzymes. In addition, we compare three NiFeS active sites and their protein environment and show that they share a significant number of structural features. We also comment on possible catalytic mechanisms.

Keywords Acetyl coenzyme A synthase · Carbon monoxide dehydrogenase · Geochemical theory of the origin of life · Hydrogenase · NiFeS-enzymes

1 Introduction

Many anaerobic microorganisms can use CO or CO_2 as a sole source of carbon and CO and/or H_2 for the generation of energy [1]. Thus, acetogens generate acetyl coenzyme A, an activated acetic acid that serves as a "universal" precursor for the generation of biomass (see below), and acetic acid from

two CO_2 molecules [2]. Carboxydotrophic bacteria oxidize CO to CO_2 generating two reducing equivalents [3] but CO_2 is also used by methanogens as the final electron acceptor [4]. The above reactions are coupled to the generation of either a Na^+ or H^+ gradient across the cytoplasmic membrane [5–7]. The ion gradient may be then either converted to chemical energy as ATP or be used to drive endergonic reactions such as the synthesis of acetyl-coenzyme A. The latter is generated directly in the supposedly very ancient Wood/Ljungdahl pathway of carbon fixation [1, 8] that is used by acetogens:

$$2CO_2 + HSCoA + 4H_2 \rightleftharpoons CH_3COSCoA + 3H_2O\,. \quad (1)$$

The central enzyme of this pathway is the bifunctional carbon monoxide dehydrogenase/acetyl coenzyme A synthase (CODH/ACS). The CODH active site catalyzes the reduction of CO_2 to CO ($E^{0'} = -512$ mV):

$$CO_2 + 2H^+ + 2e^- \rightleftharpoons CO + H_2O\,. \quad (2)$$

When the CO concentration is kept very low, as observed under normal turnover conditions of CODH/ACS [9, 10], H_2 may be used as the electron donor, after its oxidation by a hydrogenase ($E^{0'} = -414$ mV):

$$H_2 \rightleftharpoons 2H^+ + 2e^-\,. \quad (3)$$

ACS takes up the CO produced by CODH to catalyze the non-redox reaction:

$$CH_3{}^+ + CO + SCoA^- \rightleftharpoons CH_3COSCoA\,. \quad (4)$$

The methyl cation is derived from a second CO_2 molecule through a series of two-electron reduction reactions mediated by tetrahydrofolate-containing enzymes.

The active sites of CODH and ACS contain NiFeS clusters that are somewhat similar to the active site of [NiFe]-hydrogenase [11]. It has been noted recently that these biological NiFeS clusters resemble the Ni-containing form of the mineral greigite, which has been assigned an important role in the geochemical theory of the origin of life [12]. Because thiolate-ligated [4Fe – 4S] clusters form spontaneously from a solution of $FeCl_2$, HS^- and $HOCH_2CH_2SH$ [13], it is tempting to postulate that such mineral clusters were incorporated into oligopeptides that predated CODH, ACS and [NiFe]-hydrogenase. Here we will (i) discuss the origin of mineral FeS and NiFeS clusters and their catalytic properties within the context of carbon fixation as activated acetic acid; and (ii) compare these centers to those found in the highly complex extant enzyme active sites.

2 Mineral FeS and NiFeS Clusters

The conditions under which life on Earth first developed are currently assumed to have been very harsh, so that the only suitable place for the origin of life may have been the ocean floor [14]. Very hot (> 350 °C) acidic springs were a source of Ni(II) and Fe(II) sulfides, most of which, because of the almost total absence of O_2, would have remained in solution in the HCO_3^--containing acidic ocean. Wächtershäuser has proposed that the exergonic formation of pyrite from FeS provided a source of reducing power for life emergence [15]:

$$FeS + H_2S \rightleftharpoons FeS_2 + H_2(g)\,. \tag{5}$$

The reported standard free energy (ΔG^0, at 25 °C) of this reaction is − 38.4 kJ/mol [16]. Pyrite-pulled metabolism would have required acidic pH and a high H_2S concentration. In experiments carried out under such conditions, in the presence of pyrrhotite ($Fe_{1-x}S$) at 50–100 °C, CH_3SH was generated from CO_2 and H_2S [17]. After H_2 production through pyrite formation as in Eq. 5 the reaction may be written as:

$$CO_2 + H_2S + 3H_2 \rightleftharpoons CH_3SH + 2H_2O\,. \tag{6}$$

Subsequently, it was observed that an equimolar amount of precipitated NiS and FeS catalyzed the formation of acetate from CO and CH_3SH at 100 °C with an optimal pH of 6.5 [18], which is slightly basic at this temperature [19]:

$$CH_3SH + CO + H_2O \rightleftharpoons CH_3COO^- + H^+ + H_2S\,. \tag{7}$$

In addition, a small amount of the thioester CH_3COSCH_3 was also formed, which was proposed to act as an activated acetic acid intermediate in the mechanism of Eq. 7, in analogy with the formation of acetyl-CoA catalyzed by ACS (Eq. 1). In the absence of Ni no reaction was observed, indicating that Fe alone does not afford carbon fixation under the reported conditions. Table 1 shows the free energies of these and other selected reactions.

More recently, iron sulfide has been shown to play a catalytic role in the synthesis of pyruvate from alkyl thiols and carbon monoxide at 250 °C and pressures between 500 and 2000 bar (conditions that could be found at the bottom of the ocean or in a shallow oceanic crust) [20]. The overall reaction may be written as:

$$CH_3SH + 2CO + H_2O \rightleftharpoons CH_3COCOO^- + H^+ + H_2S + H_2\,. \tag{8}$$

A number of carbonylated organometallic intermediates were also detected. The solubility of CO is greatly increased at high pressure and this may favor reaction Eq. 8. Although the overall reaction is exergonic (Table 1), the yield of pyruvate, which plays a central role in many biosynthetic pathways, was

Table 1 Free energies of reactions involving simple carbon compounds

Reaction	$\Delta G^{0'}$ (kJ/mol) [a]	ΔG (kJ/mol) [b]
$2CO_2 + HSCoA + 4H_2 \rightleftharpoons CH_3COSCoA + 3H_2O$	– 146.7	– 45.7
$CH_3COSCoA + H_2O \rightleftharpoons HSCoA + CH_3COO^- + H^+$	– 35.7	– 52.8
$CO_2 + H_2S + 3H_2 \rightleftharpoons CH_3SH + 2H_2O$	– 121.3	– 52.0
$CH_3SH + CO + H_2O \rightleftharpoons CH_3COO^- + H^+ + H_2S$	– 72.2	– 70.5
$CH_3SH + 2CO + H_2O \rightleftharpoons CH_3COCOO^- + H^+ + H_2S + H_2$	– 39.5	– 37.8
$CO + H_2O \rightleftharpoons CO_2 + H_2$	– 11.1	– 23.9
$2CO_2 + 4H_2 \rightleftharpoons CH_3COO^- + H^+ + 2H_2O$	– 182.4	– 98.5
$CO_2 + 4H_2 \rightleftharpoons CH_4 + 2H_2O$	– 193.7	– 126.6
$CO_2 + H_2 \rightleftharpoons HCOO^- + H^+$	– 22.5	– 7.9
$CH_3COO^- + H^+ \rightleftharpoons CO_2 + CH_4$	– 11.3	– 28.1
$3CO_2 + 5H_2 \rightleftharpoons CH_3COCOO^- + 3H_2O + H^+$	– 156.6	– 41.0
$CH_3COO^- + CO_2 + H_2 \rightleftharpoons CH_3COCOO^- + H_2O$	25.8	57.5

[a] Standard free energy (25 °C, 1 bar, pH 7, 1 molar activities and unit activity for pure water) calculated from tabulated free energies of formation of the reactants [19, 146, 147], corrected for pH 7 (where appropriate): $RT\ln 10^{-7} = -39.9$ kJ/mol. Note that a 1 M concentration for the dissolved gases is only possible at pressures much higher than 1 bar.
[b] Calculated free energy ($\Delta G = \Delta G^0 + RT\ln K$) at pH 7 and 25 °C at physiologically more relevant activities (taking gas solubility into account) at 1 atm: $[CO_2] = 5.6$ mM, $[H_2] = [CO] = 0.5$ mM, $[CH_4] = 0.2$ mM, $[CH_3COO^-] = [H_2S] = [HCOO^-] = [CH_3SH] = [CH_3COCOO^-] = [CH_3COSCoA] = [HSCoA] = 1$ mM.

very low. The potential of various transition metal sulfides to fix carbon was tested under similar conditions [21], using the following reaction:

$$CH_3(CH_2)_8SH + CO + H_2O \rightleftharpoons CH_3(CH_2)_8COOH + H_2S\,. \quad (9)$$

The highest yields of the decanoate product were observed with nickel and cobalt sulfides, but significant activity was also observed with pyrite. In addition, the formation of methyl nonyl sulfide was observed with the methyl group originating from the reduction of CO. In this case, copper and iron sulfides were the most effective catalysts. It should be noted, however, that many important bio-molecules, such as thioesters and nucleic acids, are unstable in hot water, making some aspects of the evolution of life as we know it highly unlikely at high temperatures.

Russell and co-workers [14] have argued that the metal sulfides providing putative catalytic surfaces for abiotic carbon fixation would not have precipitated from the solutions that emanated from hot acidic springs into the equally acidic and anoxic ocean. Instead, a moderate temperature alkaline spring would have provided much more likely substrates for the emergence of

life [22]. Alkaline springs originate from the convection of ocean water within a hot ocean crust containing minerals such as $MgFeSiO_3$ (orthopyroxene) and $CaMg_6FeSi_{12}O_{24}$ (diopside). Their reaction with water forms $Mg_3Si_2O_5(OH)_4$ (serpentine), SiO_2 (silica), Fe_3O_4 (magnetite), OH^- and H_2. Reaction of another mineral, olivine ($MgFeSiO_4$), with ocean water yields similar products:

$$3MgFeSiO_4 + 4H_2O \rightleftharpoons 3SiO_2 + Fe_3O_4 + 3Mg^{2+} + 6OH^- + H_2\,. \qquad (10)$$

The resulting alkaline and reducing fluid dissolves sulfide minerals present in the crust and, consequently, these hydrothermal systems carry high concentrations of HS^-. Precipitation of HS^- with Fe(II) present in the ocean would have led to the formation of bubbles of hydrothermal fluid enclosed by semi-permeable membranes consisting mainly of FeS. Simple compounds such as CO, CN^-, NH_3, CH_3SH and HCHO would have been significant additional constituents of the hydrothermal fluid, which upon mixing with CO_2-containing ocean water provided the building blocks for pre-biotic reactions. The FeS membranes would have separated a mildly oxidizing acidic ocean solution from a reducing alkaline spring solution, thus creating a gradient in the form of both a proton motive force and an electrostatic potential. This is postulated to have provided favorable conditions for endergonic reactions to occur, as in living cells. For example, if hydrogen oxidation (Eq. 3) took place in a compartment at pH 10, the potential of the resulting electrons would be low enough to reduce CO_2 (Eq. 2) in another compartment at pH 6, assuming the existence of a conducting FeS membrane between the two compartments. Because all these reactions would have taken place within the iron-sulfur vesicles, a rapid escape of products would have been prevented, thereby allowing the gradual formation of more complex molecules [23].

Although the exact structure of the proposed iron-sulfur bubbles remains undefined, FeS should have initially precipitated as disordered mackinawite [24]. This is a highly reactive phase, which gradually converts to more stable species such as greigite (Fe_3S_4) and pyrite (FeS_2). The latter mineral plays a prominent role in Wächtershäuser's theory of pyrite-pulled surface metabolism [25] but it is not expected to be a good catalyst, because in its crystal structure each Fe(II) is bound by six sulfur pairs [26] and the resulting octahedral coordination does not leave room for an additional ligand to iron. However, surface defects in the crystal lattice could liberate metal-binding coordination sites with catalytic potential. Because aldehydes seem both to inhibit pyrite formation and enhance greigite formation [27], and simple aldehydes were plausible components of the hydrothermal fluid, it has been postulated that the iron-sulfur membranes contained at least a fraction of greigite. In this respect it is also interesting to note that both mackinawite and greigite, but not pyrite, are found in present-day magnetotactic bacteria [28]. Other metals such as nickel and cobalt may also have been incorporated into the pre-biotic FeS membrane structures. For example, in the presence of nickel, greigite may be converted from the Fe_3S_4 to the $NiFe_5S_8$

form [29]. In the laboratory, synthesis of peptide bonds in the presence of CO has been observed under alkaline conditions in the presence of a FeS/NiS mixture of, however, ill-defined structure [30].

In conclusion, many of the conditions required to support reactions resembling those taking place in extant metabolism may have existed near the ocean floor of the early Earth. Obviously, the emergence of life would have involved many other reactions and, more importantly, their regulation. The fact is that, although there are many theories about the origin of life (e.g. [31–33]), very little is actually understood about its initial conditions [34]. At any rate, there are surprising similarities between some of the molecules arising from the abiotic chemistry discussed above and the NiFeS active sites of enzymes that function in anaerobic autotrophic carbon fixation. These sites will be the subject of the following reviews.

3
NiFeS Clusters in Enzymes

Three enzymes are known to use NiFeS active sites to catalyze reactions that involve simple, primordial, gases: carbon monoxide dehydrogenase (CODH) reduces CO_2 to CO (Eq. 2, see introduction), acetyl coenzyme A synthase (ACS) combines CO with a methyl group (Eq. 4) and NiFe hydrogenase oxidizes H_2 (Eq. 3). Depending on either the organism or the physiological requirements, these enzymes can catalyze the reverse reactions as well. In acetogens like *Moorella (M.) thermoacetica*, ACS and CODH constitute the α and β-subunits of an $\alpha_2\beta_2$ bi-functional enzyme complex (see [35] and references therein) that catalyzes the sum of Eqs. 2 and 4:

$$CO_2 + CH_3{}^+ + SCoA^- + 2H^+ + 2e^- \rightleftharpoons CH_3COSCoA + H_2O\,. \tag{11}$$

In methanogens like *Methanosarcina thermophila,* they are part of the so-called acetyl-CoA decarbonylase/synthase (ACDS) $(\alpha\beta\gamma\delta\varepsilon)_8$ multi-enzyme complex that allows these organisms to grow on acetate, after it is first converted to acetyl-CoA:

$$\begin{aligned} &CH_3COSCoA + H_4SPt + H_2O \\ &\rightleftharpoons SCoA^- + CO_2 + CH_3 - H_4SPt + 2H^+ + 2e^-\,. \end{aligned} \tag{12}$$

H_4SPt is the tetrahydrosarcinapterin cofactor. The $\alpha_2\varepsilon_2$ units correspond to CODH, β is ACS, $\gamma\delta$ is a corrinoid cobalt-containing iron–sulfur protein (CoFeSP) that transfers a methyl group to H_4SPt. The electron acceptor is a ferredoxin (see [36] and references therein). A similar complex is used by obligate chemo-autotrophic methanogens, such as *Methanococcus jannaschii*, to catalyze the formation of acetyl-CoA from CO_2 and H_2 in the reverse reaction [35].

Methanogens from the genus *Methanosarcina* have one soluble and two membrane-bound [NiFe] hydrogenases [6, 37]. The latter are probably involved in energy conservation through the generation of a proton gradient. The acetogen *M. thermoacetica* may also contain several hydrogenases, but they have not been well characterized [2]. The presence of several hydrogenases is typical of a large number of microorganisms [38] and in many cases they are directly associated with other enzymes. An example of this is the coupling of CO oxidation and H_2 production by a [NiFe] hydrogenase and CODH in *Carboxydothermus (C.) hydrogenoformans* [39] and *Rubrivivax (R.) gelatinosus* [7]:

$$CO + H_2O \rightleftharpoons CO_2 + H_2\,. \tag{13}$$

Here, we will focus on those NiFe-containing enzymes for which crystal structures have been reported.

3.1 [NiFe] Hydrogenases

Heterodimeric [NiFe]-hydrogenase crystal structures have been reported for four closely related sulfate-reducing bacteria from *Desulfovibrio* sp.: *D. gigas* [40, 41], *D. vulgaris* (Miyazaki) [42–44], *D. fructosovorans* [45, 46] and *D. desulfuricans* [47]. Overall, the structures are very similar being roughly

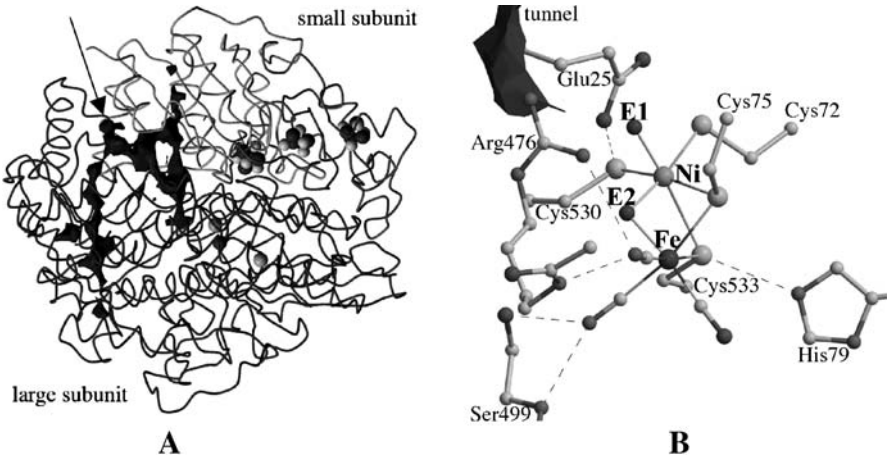

Fig. 1 Structure of [NiFe]-hydrogenase. **A** Polypeptide fold. The *arrow* indicates a hydrophobic tunnel network, shown in *dark grey*. Spheres highlight metal and inorganic sulfur sites: three FeS clusters in the small subunit and a Mg-site as well as the Ni – Fe active site in the large subunit. **B** Zoomed depiction of the active site, shown as a ball-and-stick model. *Dashed lines* indicate putative H-bonds. Exogenous ligand binding sites are labeled E1 and E2

spherical with a radius of about 35 Å (Fig. 1A). The NiFe active site is located close to the molecular center in the large subunit, which also contains a cation site close to the surface (either Mg or Fe, see below). A water ligand to the cation may be involved in a putative proton transfer pathway after molecular hydrogen cleavage from the active site, according to Eq. 3 [48]. The small subunit transfers electrons between the active site and the molecular surface through a proximal [4Fe – 4S], a median [3Fe – 4S] and a distal [4Fe – 4S] cluster. The structure of the related [NiFeSe]-hydrogenase of *Desulfomicrobium (Dm.) baculatum* shows several differences [49]: (i) a [4Fe – 4S] cluster replaces the median [3Fe – 4S] cluster of the other enzymes; (ii) a selenocysteine replaces a terminal cysteine ligand to the active site Ni; and (iii) Fe replaces Mg in the large subunit. A remarkable feature, common to the five enzymes of known structure, is the presence of a conserved, largely hydrophobic, tunnel network connecting the active site to several sites at the molecular surface. Crystal xenon-binding experiments, and subsequent molecular dynamics simulations, have shown that these tunnels are likely to provide access (and exit) pathways for H_2 gas [45].

The active site Ni and Fe ions are bridged by two cysteine thiolates. The Ni also has two additional terminal cysteine thiolate ligands, leaving two sites, here called E1 and E2, potentially available for exogenous molecules (Fig. 1B). The terminal E1 site is *trans* to the apical thiolate ligand and perpendicular to the plane defined by the three other S ligands, whereas the E2 site lies in this plane and bridges Ni and Fe. An exogenous Ni – Fe bridging ligand has only been observed in unready and ready states of oxidized inactive enzyme where it has been assigned to either an oxygen species (OH^- or OOH^-) [50, 51] or a sulfur atom [42, 47]. There is also recent evidence for a chemical modification of up to two of the active site cysteine ligands [50, 51], but it remains to be determined whether this could be due to radiation damage. A combination of crystallographic [41, 46] and FTIR spectroscopic data [52–55] has shown that the Fe ion binds one CO and two CN^- molecules. These two non-exchangeable endogenous ligands are also found in Fe-only hydrogenases [56–58] and, more recently concerning only CO, in the iron-sulfur cluster-free hydrogenase [59]. CO is also a competitive inhibitor of hydrogenases and exogenous CO has been shown to bind terminally to the Ni E1 site [44]. Special EPR techniques have detected H_2 as a bridging ligand in the H_2-sensing hydrogenase from *Ralstonia (R.) eutropha* [60], thus confirming our initial speculation based on the first hydrogenase crystal structure that E2 could bind a hydrogen species [40].

The presence of CN^- and CO ligands of the active site Fe raises the question as to how these potentially toxic molecules are incorporated in the enzyme. Significant progress has been made in the elucidation of the biosynthetic pathway of cyanide from a carbamoyl phosphate precursor [61]. On the other hand, the origin of the CO ligand remains unclear [62]. Many proteins are involved in the biosynthesis and the maturation of the active site of [NiFe]-

hydrogenases, but their specific roles have not yet been completely elucidated. For more details on these interesting aspects, the reader is referred to a recent review by Vignais and Colbeau [63].

A wealth of spectroscopic (EPR, FTIR, Mössbauer, XAS), kinetic and mutated enzyme data has been published concerning the Ni – Fe active site and many review articles are available (e.g. [11, 48, 64–72]). In addition, many density functional theory (DFT) studies of the Ni – Fe active site have been reported, but consensus on the nature of the various structures and on the catalytic mechanism is lacking (e.g. [73–79]). These theoretical studies will not be further discussed here.

A summary of most of the known states of standard [NiFe] hydrogenases and their proposed relationships is depicted in Fig. 2. Four $S = 1/2$ paramagnetic states have been detected by EPR; they are called Ni – A, Ni – B, Ni – C and Ni – L because the spin density is mainly localized on the Ni. Five diamagnetic states, called Ni – SU, Ni – "S", Ni – SI, SI – CO and Ni – R, have been characterized by FTIR, thanks to the vibration bands of the triple bonds in the CO and CN^- ligands found in the 1900–2100 cm^{-1} range. The active Ni – C and Ni – R states are directly involved in the catalytic cycle whereas the unready Ni – A and Ni – SU states are inactive and require a long reductive activation. The ready Ni – B and Ni – SI states are also inactive but can be immediately activated by H_2 in the absence of O_2. An additional active

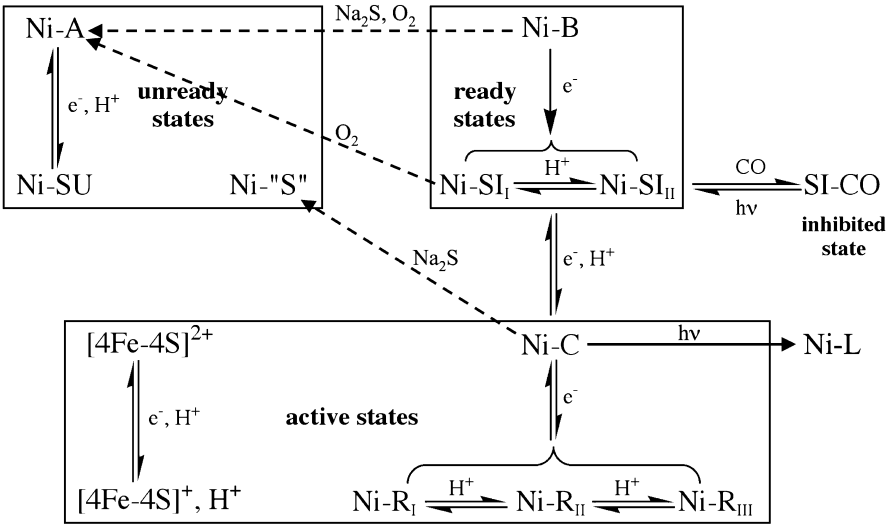

Fig. 2 Overview of the stable intermediates of [NiFe]-hydrogenase. The EPR-silent Ni – "S" state is obtained by treating active enzyme anaerobically with Na_2S [80]. Aerobic treatment of the ready Ni – B state with Na_2S leads to its conversion to the unready Ni – A state [51]. The unready state can also be obtained by addition of O_2 to enzyme in a Ni – SI state and with a reduced [3Fe – 4S] cluster (e.g. [148])

Ni – SI state with an FTIR spectrum identical to that of ready enzyme has also been characterized (not shown) [80]. The paramagnetic Ni – L state is obtained upon photolytic cleavage of the bound putative hydrogen species of the Ni – C species. Finally, SI – CO is a CO-inhibited state (e.g. [81, 82]). The picture is further complicated by the presence of different protonation states in some of these stable intermediates [54, 80] and by more than one Ni – L species [83].

Synthetic chemists have tried for many years to obtain simple structural and functional models of hydrogenases, but with limited success, especially in the case of the [NiFe] enzymes (see [84–86] for recent reviews). One possible reason for this situation is the difficulty in obtaining stable complexes with two orthogonal (*cis*) Ni empty coordination sites, a characteristic of the active site of all the [NiFe] hydrogenase crystal structures reported so far. Another problem for biomimetic modeling is the tendency of thiolates to bridge metal ions, leading to the formation of polynuclear clusters. On the other hand, good progress has been made in the understanding of the redox properties of Ni and the modeling of the iron center and its ligands. Furthermore, many of the properties of [NiFe] hydrogenase biomimetic models may also be relevant for the NiFeS active sites of CODH and ACS discussed below.

3.2
Nickel-Containing Carbon Monoxide Dehydrogenases

Four crystal structures of Ni CODHs have been determined from the following organisms: *C. hydrogenoformans* [87, 88], *Rhodospirillum (R.) rubrum* [89] and the bifunctional CODH/ACS from *M. thermoacetica* [90, 91]. In each case CODH has a very similar homodimeric quaternary structure with a diameter of about 100 Å in the largest dimension and a total of five FeS clusters (Fig. 3A). An initially unexpected [4Fe – 4S] center, now called the D-cluster, is coordinated by the two subunits very close to the molecular surface. Each subunit also binds an additional [4Fe – 4S] center, called the B-cluster, as well as the catalytic Ni-containing C-cluster. There is an electron transfer pathway between the physiological redox partner, the exposed D-cluster, then the B-cluster of one subunit and finally the C-cluster of the other subunit. The electron flow direction will depend on whether the enzyme reduces CO_2 or oxidizes CO (Eq. 2).

Putative pathways have been characterized in *C. hydrogenoformans* CODH for the respective transit of CO/CO_2 and the H_2O product through hydrophobic and hydrophilic tunnels, respectively [87]. The bi-functional CODH/ACS from *M. thermoacetica* contains several hydrophobic tunnels that connect the two CODH C-cluster active sites to each other and to the ACS active site named the A-cluster [90]. High-pressure, xenon-binding experiments carried out in a CODH/ACS crystal have shown that these tunnels can trap many xenon atoms [91]. In addition, putative proton transfer pathways connecting

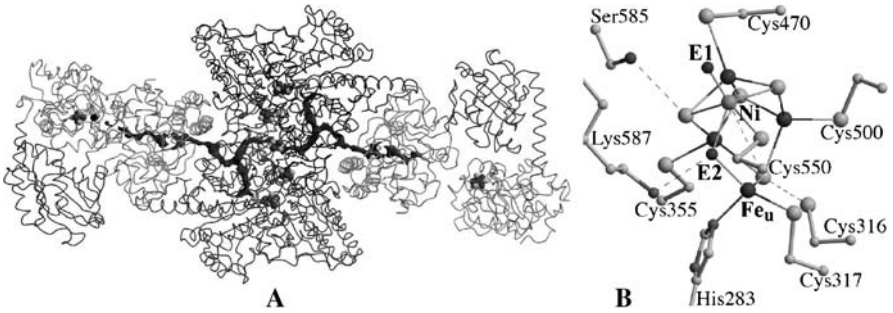

Fig. 3 Structure of the carbon monoxide dehydrogenase/acetyl coenzyme A synthase (CODH/ACS) hetero-tetramer. **A** Polypeptide fold of the CODH dimer (*center*) and of ACS in the closed (*left*) and open subunit conformation (*right*). Metal sites and inorganic sulfurs are shown as *spheres*; an extensive hydrophobic tunnel network is highlighted in *dark grey*. **B** Zoomed depiction of the CODH active site. *Dashed lines* indicate putative H-bonds

the C-cluster to the molecular surface have been proposed using site-directed mutagenesis [92].

The catalytic C-cluster consists of a [3Fe – 4S] sub-site linked through three labile S^{2-} ions to a Ni – Fe site (Fig. 3B): two of these sulfides are ligands to the Ni ion, whereas the third one binds the unique Fe (Fe_u), which is further coordinated by a histidine imidazole and a cysteine thiolate ligand. Given its unusual configuration, Fe_u most likely corresponds to the Ferrous Component II (FCII) defined by Mössbauer spectroscopy [93]. In addition, the Ni and the Fe ions of the [3Fe – 4S] sub-site are bound to the protein through cysteine thiolates. We have recently analyzed the available C-cluster structures and have found some differences that are most likely due to dissimilar conditions in the growth, purification and subsequent treatment of the enzymes [94]. In the structure of *R. rubrum* CODH, the Ni cysteine ligand also binds to Fe_u [89] at a site here called E2 by analogy with [NiFe]-hydrogenases (see above). In the *C. hydrogenoformans* enzyme, E2 is occupied by an exogenous bridging atom, modeled as a fifth inorganic S atom, which disappeared when the enzyme was treated with excess CO [88]. Because this treatment also resulted in loss of activity, it was argued that structures that lack the fifth labile sulfide are non-functional. However, Lindahl and co-workers [95] have shown that the addition of exogenous sulfide as Na_2S leads to the reversible inhibition of *R. rubrum* and *M. thermoacetica* CODHs. In fact, the bridging sulfide of *C. hydrogenoformans* CODH could be a SH^-, resulting from the reduction of COS, which is an alternative substrate of CODH [96]:

$$COS + H^+ + 2e^- \rightleftharpoons CO + SH^- . \tag{14}$$

Like the Ni ion in hydrogenase, the C-cluster Ni has two *cis* binding sites available for exogenous ligands: a Ni – Fe bridging E2 site and a terminal E1 site. Also as in hydrogenases, E1 points to the end of a hydrophobic tunnel. In

a CO-treated crystal of *M. thermoacetica* CODH/ACS E1 is occupied by a ligand that was tentatively assigned to a partially occupied CO molecule [91].

Several different stable active site intermediates of the C-cluster have been reported (see [97] and references therein). Gradual reduction of the oxidized enzyme results in the following species, as characterized by EPR spectroscopy: an initial diamagnetic inactive C_{ox} state, a paramagnetic C_{red1}, a putative diamagnetic C_{int} and a paramagnetic C_{red2} state. It is generally assumed that the two paramagnetic states are involved in catalysis, with C_{int} being a hypothetical intermediate between C_{red1} and C_{red2}. In addition, a large number of substrate and inhibitor complexes have been characterized. Many CO-bound states and putative formate or CO_2 complexes were detected in a recent FTIR study of CO binding to CODH/ACS of *M. thermoacetica* [98]. No high frequency bands were detected in the untreated enzyme, thus excluding the presence of intrinsic CO, as was proposed for the *R. rubrum* enzyme [99].

Several small molecules bind to the C_{red1} but not to the C_{red2} state, providing EPR-detectable paramagnetic species. These include CN^- [100, 101], SCN^-, OCN^-, N_3^- [102], SH^- [95] and CS_2 [103]. The electronic structure and binding mode of the tri-atomic anions SCN^-, OCN^- and N_3^- (EPR g_{av} between 2.15 and 2.17) differ from those of the C_{red1} and C_{red2} states and the other inhibitor complexes (EPR g_{av} between 1.66 and 1.86). In the latter, the unpaired electron appears to be localized mainly in the [3Fe – 4S] sub-site (see [97] and references therein). The crystal structures of most of the spectroscopically characterized C-cluster intermediates and complexes remain to be determined. The high temperature factors of many of the C-cluster atoms and ligands in the known structures suggest a substantial degree of disorder that may be due to the presence of a mixture of states in the crystals. Unfortunately, it has been generally difficult to obtain well-diffracting crystals of homogeneous states.

3.3
Acetyl Coenzyme A Synthases

Three crystal structures of ACS have been reported, two of CODH/ACS from *M. thermoacetica* [90, 91] and one of the monomeric ACS from *C. hydrogenoformans* [104]. ACS consists of three globular domains with the catalytic A-cluster bound to domain 3 at its interface with domain 1. As mentioned above, CODH/ACS has a hydrophobic tunnel network that allows CO, the product of Eq. 2 catalyzed by the C-cluster, to diffuse to the A-cluster where it combines with the methyl group donated by CFeSP to form an acetyl group that, in turn, binds to coenzyme A (Eq. 4). The presence of a tunnel connecting the two active sites was predicted before the structure was determined because, under normal turnover conditions, no CO was detected in the reaction medium [9, 10].

In the crystal structure determined by Doukov et al. the A-cluster was relatively buried and a change of ACS to a more open conformation was proposed to allow access of the methyl group and coenzyme A to the active site [90]. An open form was subsequently observed in one of the ACS subunits of the structure of a different crystal form of the same enzyme (the other sub-unit was in the already known closed conformation) [91] (Fig. 3A). A similar open form was later observed in the *C. hydrogenoformans* ACS crystal structure [104]. The rearrangement of the structure involves a rigid body rotation of domains 2 and 3 with respect to domain 1, which packs against the CODH dimer. In the open form, the movement of an α-helix of domain 1 blocks the tunnel to the A-cluster. We have proposed that these conformational changes provide a gating mechanism for access of substrates to the A-cluster when ACS is in its closed form that prevents CO leakage to the environment [105]. We also proposed that CO_2 could access the enzyme through the A-cluster and then travel to the C-cluster through the hydrophobic tunnels. In CODH/ACS mutants with a blocked tunnel, most of the ACS activity was lost in the presence of CO_2 and a reducing agent, confirming the important role of the tunnel in providing CO access to the A-cluster [106]. On the other hand, the CODH activity was not significantly affected, suggesting that other, so far undetected and maybe transient pathways allow diffusion of CO/CO_2 to and from the C-cluster.

The A-cluster consists of a standard [4Fe – 4S] cluster connected through one of its cysteine ligands to a proximal metal ion that is, in turn, bridged through two additional cysteine thiolates to a distal Ni ion (Ni_d). The crystal structures have shown that this metal ion can be Cu [90], Zn [91] or Ni [91, 104]. Cu and Zn are observed in the closed ACS conformations and Ni in the open ones (Fig. 4A). Following these observations, there was a short-lived debate as to which of these metals is part of the physiologically relevant active site (e.g. [107–111]). Currently, there is a consensus that the proximal active metal is Ni_p [91, 104, 112], as indicated by recent results obtained with the ACS subunit from the *Methanosarcina thermophila* ACDS complex [113, 114] and by an earlier finding that activity positively correlates with the presence of a labile Ni ion [115]. The labile nature of the catalytic Ni originates from its significant solvent exposure in the ACS open form. This has been confirmed by the recent observation that Zn can replace Ni_p at the A-cluster only during turnover, when ACS probably alternates between the closed and open forms [116].

Ni_d has square planar coordination involving two bridging cysteine thiolates and two main chain N atoms (Fig. 4A). A similar structure has been described recently for the active site of nickel superoxide dismutase (NiSOD) [117, 118] (Fig. 4B). In NiSOD, Ni(II) reacts with superoxide and is oxidized to Ni(III)-peroxide. On the other hand, ACS functions in reducing environments and Ni_d is thought to remain as Ni(II) throughout catalysis. Model chemistry supports this proposal indicating that Ni_p is much more

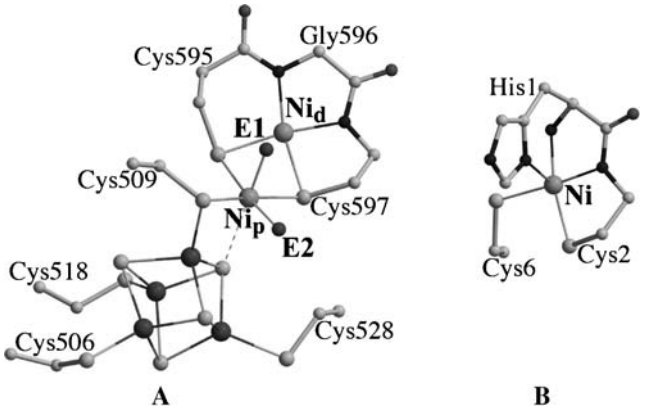

Fig. 4 **A** Active site of acetyl coenzyme A synthase (ACS). **B** Active site of Ni-superoxide dismutase (Ni – SOD)

likely to be reduced than Ni_d (for reviews see [119–122]). Reaction of the A-cluster with CO generates a paramagnetic species that has been assigned to a Ni(I) – CO complex. Isotopic substitution with ^{61}Ni, ^{13}CO or ^{57}Fe results in line broadening of the EPR spectrum and, consequently, the CO complex has been called the NiFeC species [123]. The isotopic effects can be best explained if the EPR signal arises from a proximal Ni(I) with bound CO.

In the open ACS conformation of *M. thermoacetica* CODH/ACS, Ni_p has square planar coordination involving three cysteine thiolates and an unidentified exogenous ligand at the E2 site that could correspond to either formate or SO_2 [105, 124]. Although these putative ligands are probably not functionally relevant, they underline the propensity of the E2 site to bind exogenous molecules directly from the solvent. An apical fifth potential coordination site, called E1, is *trans* to one of the labile S atoms of the [4Fe – 4S] cluster and points towards Phe512. A residual electron density peak close to this site, at 1.3 Å from the square planar Ni_p, suggests that a small fraction of the metal at the proximal site adopts a tetrahedral coordination, as already observed for both proximal Cu and Zn in the closed ACS conformation [90, 91]. This would require a rotation of Phe512, which is, as a matter of fact, partially disordered. We have not been able to identify the metal that occupies the minor tetrahedral site in the open ACS due to its low occupancy. In conclusion, Ni_p, like the Ni ions in [NiFe] hydrogenases and the C-cluster of CODH, has two *cis*-coordination sites available for substrate binding, although in this case both open sites are terminal as it may be required for the insertion/migration reaction of acetyl synthesis.

4 Catalytic Mechanisms

The structural similarities between the active sites of [NiFe]-hydrogenase, CODH and ACS suggest that the respective catalytic mechanisms may be similar as well. In each case, a hydrophobic tunnel points to the Ni apical E1 coordination site providing access and exit pathways for gaseous substrates and products. In addition, an orthogonal E2 site is also available for binding exogenous ligands. In CODH and hydrogenase, E2 is also a coordination site for the Fe ion. Although the structural differences between the three active sites are likely to be very important in determining the nature of the reaction, the protein environment may also play a major role in determining the catalytic properties of these enzymes. For example, the A-cluster of ACS cannot catalyze net two-electron redox reactions because there is no redox center at a suitable distance and, by the same token, hydrogenases cannot oxidize CO to CO_2 because there is no water channel leading to the buried NiFe active site.

A unique feature of the two major classes of hydrogenases is the presence of structural CN^- and CO ligands to Fe [41, 53–56, 125]. Recently, the so-called FeS-free hydrogenase, for a long time considered as a metal-free enzyme, has been shown to have a cofactor containing a low-spin iron, probably Fe(II), with bound CO [59, 126]. Thus, the association of CO to Fe appears to be central to the biological metabolism of molecular hydrogen. CO is a good π-acceptor that will favor transition metal binding to soft σ-donor ligands such as hydride *trans* to it. Indeed, in both NiFe and Fe-only enzymes, CO binds *trans* to a vacant coordination site to Fe. In the former, this is the bridging E2 site that binds either hydride or H_2 in the *R. eutropha* H_2-sensing hydrogenase [60]. Several catalytic mechanisms have been proposed for standard [NiFe]-hydrogenases but no consensus has been reached. It is often assumed that the Ni – Fe bridging site E2 that is occupied by O or S species in inactive states of the enzyme corresponds to the H_2 binding site during catalysis. This is an appealing proposition because in Fe-only hydrogenases the postulated H_2 binding site is a $FeS_2(CO)_2CN$ unit that can be closely superimposed to an equivalent $FeS_2CO(CN)_2$ portion in the [NiFe] enzyme active site [58]. However, the Ni – C state, which already has a hydrogen species bound to E2, is very active in H_2 uptake [127–129]. This would imply that hydrogen binds to the terminal Ni E1 site during turnover, consistent with the observation that the competitive inhibitor CO binds at this site [44]. In this case, the putative bridging hydride at E2 would function as the first base that is required for the heterolytic cleavage of H_2. These ideas are summarized in Scheme I shown inFig. 5.

In CODH, a crucial issue is the location of the two electrons in C_{red2}, which reduces CO_2 to CO according to Eq. 2. According to Mössbauer spectroscopic results, FCII is not the species reduced during the transition from

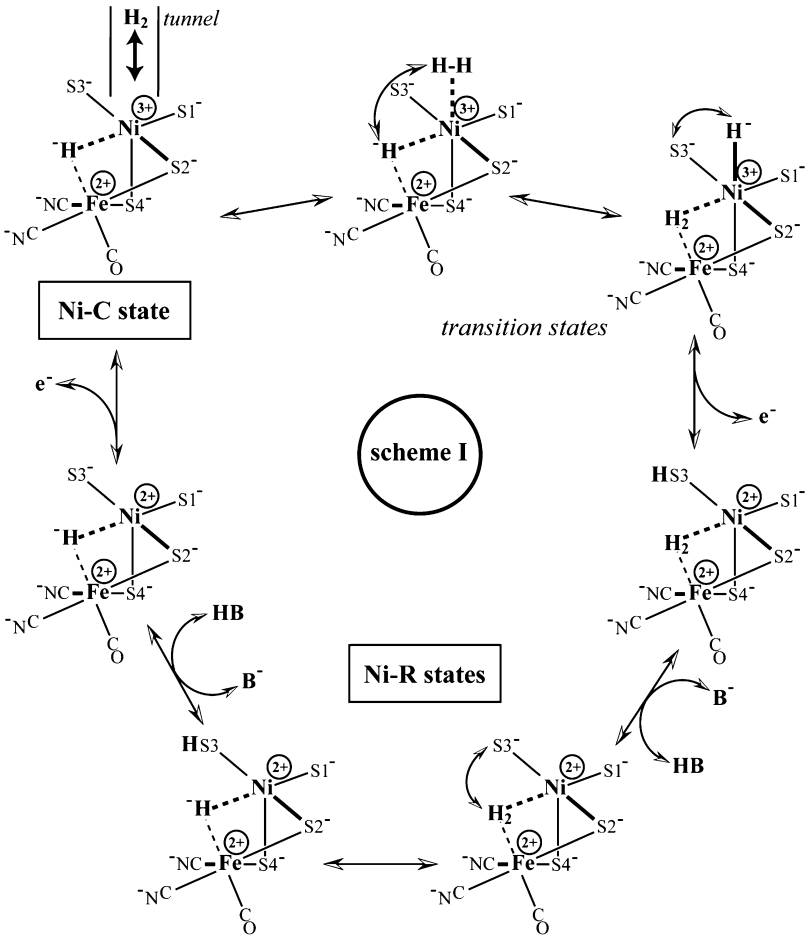

Fig. 5 Putative catalytic cycle of [NiFe]-hydrogenase. In this scheme, heterolytic H_2 cleavage at the terminal E1 site takes place simultaneously with H_2 bond formation at the Ni – Fe bridging E2 site, giving both exogenous *cis*-ligation sites of the Ni an indispensable role during catalysis. The resulting hydride at E1 immediately loses one electron to the Ni and one to the proximal cluster, whereas a nearby base that could be Cys530 accepts the remaining proton (Fig. 1B). The resulting Ni(II) – H_2 species may correspond to one of the three protonation states that have been detected for Ni – R, the most reduced stable state [80]. After proton transfer from Cys530 to Glu18, the next base in a likely pathway [130], Cys530 may assist in the heterolytic cleavage of the bridging H_2 by abstracting a proton. Finally, after electron transfer to the distal cluster, the proximal cluster may oxidize the active site to the Ni – C state, thus closing the cycle. An advantage of this scheme over others is that the bridging E2 site is always occupied, providing a stable coordination environment for the Ni ion in all the catalytic intermediates. In addition, it involves minimal conformational changes, thus allowing very rapid catalysis, in agreement with the observation that the turnover rate of the enzyme when coated on a spinning graphite electrode is limited by the rate of diffusion of H_2 to the active site [131]

the C_{red1} to the C_{red2} state [93]. In addition, neither the Mössbauer nor the UV/visible spectra are significantly different when these two states are compared, strongly suggesting that the electrons do not go to the [3Fe – 4S] subsite either [93, 132]. Another possibility is the reduction of the Ni center from Ni(II) to Ni(0). It is not clear how Ni^0 would be stabilized in the C-cluster but, if this proposition is taken only formally, the charge could be de-localized over the Ni ligands. This would agree with an XAS study of *C. hydrogenoformans* CODH that showed that the electron density at the Ni center does not change upon the two-electron reduction of the C-cluster [133]. A further scheme involves the reduction of a persulfide bond between Cys316 and an inorganic sulfur atom of the cluster, since this bond was observed as a minor component in the crystal structure of the *M. thermoacetica* enzyme [91]. Mutation of Cys316 to Ala resulted in inactive enzyme, but this turned out to be due to the loss of the C-cluster [92].

In the two known crystal structures of *M. thermoacetica* CODH/ACS, the $NiFe_u$ E2 bridging site does not display any detectable electron density [90, 91] (Fig. 3B), which apparently leaves only three protein ligands to coordinate Fe_u. Because such a paucity of ligands seems unlikely, it is possible that E2 is occupied by a hydride resulting from the two-electron reduction of a proton, which would thus result in a tetrahedrally coordinated Fe_u. This structure would then be analogous to the Ni – C state in [NiFe]-hydrogenases [60]. Indeed, a bridging hydride could explain the (low) H_2 evolution reported for CO-treated CODH in the absence of electron acceptors other than protons [98, 134]. Consequently, and mainly based on the crystal structures, we tend to favor a proton as the two-electron acceptor [94]. It should be mentioned, however, that there is also a potential problem with the hydride proposal: the absence of a strong ENDOR signal from a proton nucleus [101] is only compatible with a bridging hydride carrying no significant electron spin density. Assuming that the proton hyperfine coupling detected in the C_{red1} state is correctly assigned to a bridging hydroxide ligand [101], this would imply that C_{red2} and C_{red1} have significantly different electronic structures. Figure 6 depicts a plausible catalytic cycle involving a bridging hydride in C_{red2} (Scheme II). Similarities with the heterolytic H_2 cleavage reaction proposed in Fig. 5 include a bridging NiFe hydride and the participation of both E1 and E2 sites in the catalytic process.

Clearly many of the structural and electronic changes that occur during catalysis at the C-cluster are not yet completely understood and more studies are needed, including high-resolution structural characterizations of homogenous intermediate states of the catalytic cycle.

Although acetyl-CoA synthesis (Eq. 4), as catalyzed by the A-cluster, does not involve net electron consumption, the mechanism is thought to involve two redox steps. The first of these steps is the oxidative addition of the methyl cation that is transferred from CFeSP to Ni_p. The second redox step corresponds to the reductive elimination of the nascent acetyl group

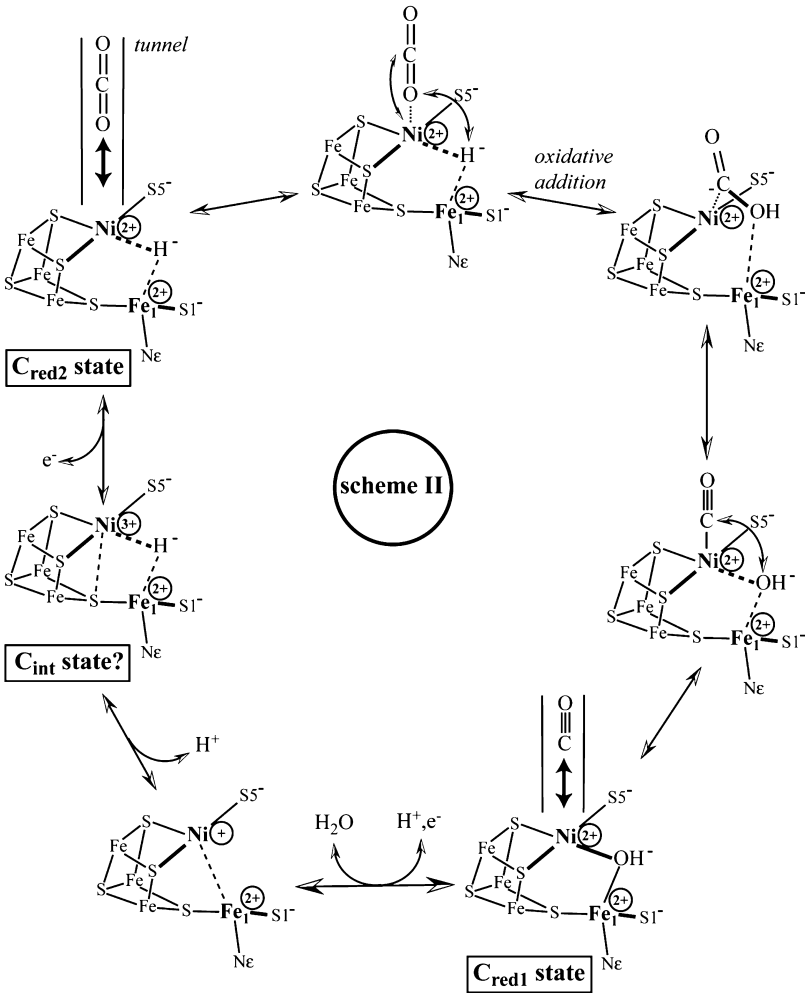

Fig. 6 Putative catalytic cycle of CODH involving a Ni – Fe bridging hydride. The bridging hydride is assumed to be stable enough to prevent its fast reaction with a proton. The reaction can be divided into several steps: 1) CO_2 binds end-on at the axial E1 site; 2) the hydride attacks the bound CO_2 forming a transient formate complex; 3) the C – OH bond is broken, generating an intermediate that has E1 occupied by CO and E2 by OH^-; 4) CO dissociates from Ni as a Ni(II)-bound axial CO is not very stable [135], generating the C_{red1} state that has a bridging hydroxide; 5) addition of two electrons via the D- and B-clusters and of two protons via a proton channel leads to dehydration and regeneration of the C_{red2} state. The hypothetical C_{int} form is depicted as having Ni(III). However, an alternative would be a species with Ni(II) and one of the cluster irons oxidized to Fe(III).

that is transferred to CoA. A crucial question concerns the identity of the two-electron donor/acceptor. Although non-redox, sulfur-based catalysis, in which the methyl cation binds to a thiolate ligand, has precedent in model

compounds (e.g. [86]), and could represent an alternative mechanism, it is generally accepted that the transferred methyl group binds to a metal ion. A redox-dependent process is in agreement with the observation that the enzyme needs to be reductively activated [97]. In the following discussion we will therefore assume metal-based catalysis analogous to the industrial Monsanto process of acetate formation.

In the Monsanto process, which operates at 30 to 60 bars and 150 to 200 °C, the catalyst $[Rh^{I}(I)_2(CO)_2]^-$ is the initial electron donor: oxidative addition of CH_3I produces a transient $[Rh^{III}(I)_3(CO)_2CH_3]^-$ state that rapidly converts to a stable $[Rh^{III}(I)_3CO(COCH_3)]^-$ acetyl intermediate upon methyl migration. Addition of another CO followed by reductive elimination of CH_3COI and a final hydrolysis step leads to the production of CH_3COOH and HI and the regeneration of $[Rh^{I}(I)_2(CO)_2]^-$ [136]. ACS catalysis in *M. thermoacetica* takes place at 1 bar and 45–65 °C [2]. Possible electron donor/acceptor sites are Ni_d, Ni_p, the [4Fe – 4S] cluster and a putative pair of cysteines that could form a disulfide bond. Another unclear point is the sequence of events in vivo, i.e. which reaction occurs first, carbonylation or methylation, although both sequences are possible in vitro.

The absence of CO leakage to the medium during CO_2 reduction at the C-cluster and acetyl-CoA formation [9, 10] indicates that, in vivo, CO arrives to the A-cluster through the hydrophobic tunnel previously discussed. Therefore, the results of experiments where CO is added externally should be interpreted with caution. The situation may be different, however, for organisms like *C. hydrogenoformans* that are able to grow on CO as a carbon and reducing power source and which have mono-functional CODH and ACS [104]. As mentioned above, upon reaction with external CO, an apparently kinetically competent paramagnetic NiFeC species is observed in both *M. thermoacetica* CODH/ACS and *C. hydrogenoformans* ACS [137, 138]. However, no other paramagnetic intermediates have been observed upon subsequent methylation and CoA acetylation, and the involvement of the NiFeC species in catalysis has been questioned [114, 139, 140]. A summary of the NiFeC species-based "paramagnetic" mechanism is shown below:

$Fe_4S_4^{2+}Ni_p^{2+} + e^- \rightarrow Fe_4S_4^{+}Ni_p^{2+}$
(*reductive activation*)

$Fe_4S_4^{+}Ni_p^{2+} + CO \rightarrow Fe_4S_4^{2+}Ni_p^{+}CO$
(*carbonylation and rapid formation of the NiFeC state*)

$Fe_4S_4^{2+}Ni_p^{+}CO + CH_3^{+} \rightarrow Fe_4S_4^{2+}Ni_p^{3+}(CO)CH_3^{-}$
(*methylation by oxidative addition*)

$Fe_4S_4^{2+}Ni_p^{3+}(CO)CH_3^{-} + e^- \rightarrow Fe_4S_4^{2+}Ni_p^{2+}(CO)CH_3^{-}$
(*rapid one-electron reduction*)

$Fe_4S_4^{2+}Ni_p^{2+}(CO)CH_3^- \rightarrow Fe_4S_4^{2+}Ni_p^{2+}(COCH_3)^-$
(*methyl migration or CO insertion*)
$Fe_4S_4^{2+}Ni_p^{2+}(COCH_3)^- + CoA^- \rightarrow Fe_4S_4^{+}Ni_p^{2+} + \text{acetyl-CoA} + e^-$
(*reductive elimination*).

This mechanism requires at least two rapid electron transfer steps and, consequently, Ragsdale and co-workers initially proposed fast intramolecular electron transfer between CODH and ACS [137]. However, this is not compatible with the long distance that separates the ACS A-cluster and the CODH redox centers [90, 91]. Under in vivo conditions another redox partner could be involved. In this scheme, it is tacitly assumed that CO is required for the first one-electron reaction as no paramagnetic species is detected upon reductive activation of the enzyme in the absence of CO [138].

Lindahl and co-workers have observed that, in vitro, acetyl-CoA synthesis may take place when methylation precedes carbonylation [140]. In this case, no stable paramagnetic state of the A-cluster, such as NiFeC, is detected by EPR. In addition, they also found that reduction of the [4Fe – 4S] cluster is slower than the methylation reaction and concluded that the former cannot be an electron donor for the latter reaction [141]. Therefore, the two electrons needed to form the CH_3 – Ni bond must come from somewhere else. One possibility involves the reduction of Ni_p to Ni^0 [91, 142]. A simplified summary of the corresponding "diamagnetic" mechanism is:

$Ni_p^{2+} + 2e^- \rightarrow Ni_p^{0}$
(*reductive activation*)
$Ni_p^{0} + CH_3^+ \rightarrow Ni_p^{2+}CH_3^-$
(*oxidative addition*)
$Ni_p^{2+}CH_3^- + CO \rightarrow Ni_p^{2+}(COCH_3)^-$
(*carbonylation + methyl migration or CO insertion*)
$Ni_p^{2+}(COCH_3)^- + CoA^- \rightarrow Ni_p^{0} + \text{acetyl-CoA}$
(*reductive elimination*).

This mechanism requires the coexistence of Ni^0 and a $[4Fe-4S]^{2+}$ center at the A-cluster. However, DFT calculations have shown that such an electronic configuration should convert to Ni^+ and $[4Fe-4S]^+$ [143]. In addition, Ni^0 would only be stable next to a reduced, EPR-active $[4Fe-4S]^+$ cluster [144], which is incompatible with the experimental results. A modification of the "Ni^0" mechanism involves two-electron transitions between a $[4Fe-4S]^{2+}Ni^{2+}/[4Fe-4S]^+Ni^+$ pair [144], against the evidence mentioned above that redox changes at the [4Fe – 4S] cluster are much slower than the turnover rate of the enzyme [141]. Involvement of an alternative $Ni_p^{2+}Ni_d^{2+}/Ni_p^{+}Ni_d^{+}$ pair is neither supported by DFT calculations nor by model chemistry [110].

Another proposed two-electron redox site involved the formation and cleavage of a disulfide bond between two cysteine residues located close to the A-cluster [140]. This proposal was initially discarded [90, 91] due to the absence of a pair of free cysteines near the A-cluster but, more recently, Svetlitchnyi and co-workers proposed that the two cysteines bridging Ni_p and Ni_d could function as a redox site [104]. Arguing against this possibility, we found that forming a disulfide bridge between these two residues is only possible after unreasonably large structural rearrangements (not shown). However, an alternative disulfide bond could be formed between Cys528, which binds one of the Fe ions of the cluster, and Cys597, through a simple rotation of the side chain of the former [105]. DFT calculations have indicated that this disulfide bond is stable in the methyl and acetyl complexes [144]. A simplified summary of a diamagnetic Cys528/Cys597 mechanism is:

$S^-S^-Ni^{2+} + CH_3^+ \rightarrow S\text{-}S\ Ni^{2+}CH_3^-$
(*oxidative addition*)
$S\text{-}S\ Ni^{2+}CH_3^- + CO \rightarrow S\text{-}S\ Ni^{2+}(COCH_3)^-$
(*carbonylation + methyl migration or CO insertion*)
$S\text{-}S\ Ni^{2+}(COCH_3)^- + CoA^- \rightarrow S^-S^-Ni^{2+} + \text{acetyl-CoA}$
(*reductive elimination*).

One challenge with this mechanism is to determine the electronic state of the A-cluster before reductive activation. Another problem is the absence of a disulfide bond between Cys528 and Cys597 in all the structures solved so far. At any rate, this proposition makes sense because it is known from model chemistry that metal ions can oxidize coordinated thiolates, leading to the formation of a disulfide bond and a reduced metal center (e.g. [122]). A sulfur-based "D-site" could also be incorporated in a paramagnetic catalytic cycle:

$S^-S^-Ni^{2+} + CO + e^- \rightarrow S^-S^-Ni^+CO$
(*reductive activation and carbonylation*)
$S^-S^-Ni^+CO + CH_3^+ \rightarrow S\text{-}S\ Ni^{2+}(COCH_3)^- + e^-$
(*oxidative addition and acetyl formation*)
$S\text{-}S\ Ni^{2+}(COCH_3)^- + CoA^- \rightarrow S^-S^-Ni^{2+} + \text{acetyl-CoA}$
(*reductive elimination*).

What is the relevance of the NiFeC species? What can be deduced, based on the closed and open ACS conformations observed in the crystal structure, is that CO is more likely to bind in the closed form, prior to methyl group binding (in the open form), than the other way round [91, 105]. This is because the tunnel is blocked in the open form and apparently there is not enough space in the closed form for the binding of a methyl group at the E2 site.

A second question is, where does CO bind when added externally? It is known that acetyl-CoA synthesis is much faster in the presence of CO_2 plus reductant than with externally added CO [145]. This argues for different initial CO binding modes in the two cases and it is conceivable that the mechanism differs depending on whether CO is added externally or it arrives through the tunnel after CO_2 reduction at the C-cluster. More studies will be required before the ACS catalytic mechanism is fully elucidated.

5 Conclusions

NiFeS clusters and the origin of life. There are currently two opposite ways of considering the origin of life on Earth. One of these proposes the formation of pre-biotic structures in a "primordial soup" rich in organic molecules originally generated by meteoric activity. The other view postulates that pre-biotic metabolisms were iron–sulfur based. In this review we have analyzed this second proposition and have compared some inorganic reactions proposed to be ancestral to those found in extant, mostly anaerobic, microorganisms. Many of the active sites of enzymes catalyzing fundamental reactions such as hydrogen oxidation or carbon fixation have NiFeS cluster structures that are reminiscent of those of nickel-containing minerals, such as greigite. Although it is conceivable that the first stages in the evolution of catalysis took place in the absence of protein, the rather sophisticated control of diffusion of substrates and products by extant enzymes suggests that metal-polypeptide associations were early components in the evolution of life. Further characterization of NiFeS-based, pre-biotic catalysis will be needed before the plausibility of a mineral-based origin of life is confirmed.

Acknowledgements We thank Siem Albracht, Patricia Amara, Bart Faber, Christine Cavazza, Marie-Hélène Charon, Claudine Darnault, Victor Fernandez, Martin Field, Michel Frey, Elsa Garcin, Claude Hatchikian, Eun Jin Kim, Antonio de Lacey, Pierre Legrand, Paul Lindahl, Lydie Martin, Michael Matho, Yaël Montet, Yvain Nicolet, Marc Rousset, Winfried Roseboom and Xavier Vernède for their important contributions to our studies of NiFeS clusters in enzymes, and Michael Russell for the stimulating discussions on pre-life conditions and non-biological carbon fixation.

References

1. Wood HG (1991) FASEB J 5:156
2. Drake HL, Daniel SL (2004) Res Microbiol 155:869
3. Ragsdale SW (2004) Crit Rev Biochem Mol Biol 39:165
4. Thauer RK (1998) Microbiol 144:2377
5. Müller V (2003) Appl Environm Microbiol 69:6345

6. Deppenmeier U (2004) J Bioenerg Biomembr 36:55
7. Maness PC, Huang J, Smolinski S, Tek V, Vanzin G (2005) Appl Environ Microbiol 71:2870
8. Ljungdahl LG (1986) Annu Rev Microbiol 40:415
9. Maynard EL, Lindahl PA (1999) J Am Chem Soc 121:9221
10. Seravalli J, Ragsdale SW (2000) Biochemistry 39:1274
11. Volbeda A, Fontecilla-Camps JC (2005) Coord Chem Rev 249:1609
12. Russell MJ, Martin W (2004) Trends Biochem Sci 29:358
13. Bonomi F, Werth MT, Kurtz DM (1985) Inrg Chem 24:4331
14. Russell MJ, Hall AJ, Boyce AJ, Fallick AE (2005) Econ Geol 100:419
15. Wächtershäuser G (1988) Syst Appl Microbiol 10:207
16. Wächtershäuser G (1990) Proc Natl Acad Sci USA 87:200
17. Heinen W, Lauwers AM (1996) Orig Life Evol Biosph 26:131
18. Huber C, Wächtershäuser G (1997) Science 276:245
19. Amend JP, Shock EL (2001) FEMS Microbiol Rev 25:175
20. Cody GD, Boctor NZ, Filley TR, Hazen RM, Scott JH, Sharma A, Yoser HS Jr (2000) Science 289:1337
21. Cody GD, Boctor NZ, Brandes JA, Filley TR, Hazen RM, Yoser HS Jr (2004) Geochim Cosmochim Acta 68:2185
22. Russell MJ (2003) Science 302:580
23. Russell MJ, Hall AJ (1997) J Geol Soc (London) 154:377
24. Wolthers M, Van der Gaast SJ, Rickard D (2003) Am Mineral 88:2007
25. Wächtershäuser G (1988) Microbiol Rev 52:452
26. Finklea SL III, Cathey L, Amma EL (1976) Acta Cryst A32:529
27. Rickard D, Butler IB, Oldroyd A (2001) Earth Planet Sci Lett 189:85
28. Posfai M, Buseck PR, Bazylinski DA, Frankel RB (1998) Science 280:880
29. Vaughan DJ, Craig JR (1978) Mineral chemistry of natural sulfides. Cambridge University Press, Cambridge
30. Huber C, Wächterhäuser G (1998) Science 281:670
31. Cody GD (2004) Ann Rev Earth Planet Sci 32:569
32. Anet FAL (2004) Curr Opin Chem Biol 8:654
33. Pereto J (2005) Int Microbiol 8:23
34. Trevors JT, Abel DL (2004) Cell Biol Int 28:729
35. Lindahl PA, Chang B (2001) Orig Life Evol Biosph 31:403
36. Grahame DA, Gencic S, Demoll E (2005) Arch Microbiol 184:32
37. Hedderich R (2004) J Bioenerg Biomembr 36:65
38. Vignais PM, Billoud B, Meyer J (2001) FEMS Microbiol Rev 25:455
39. Soboh B, Linder D, Hedderich R (2002) Eur J Biochem 269:5712
40. Volbeda A, Charon MH, Piras C, Hatchikian EC, Frey M, Fontecilla-Camps JC (1995) Nature 373:580
41. Volbeda A, Garcin E, Piras C, De Lacey AL, Fernandez VM, Hatchikian EC, Frey M, Fontecilla-Camps JC (1996) J Am Chem Soc 118:12989
42. Higuchi Y, Yagi T, Yasuoka N (1997) Structure 5:1671
43. Higuchi Y, Ogata H, Miki K, Yasuoka N, Yagi T (1999) Structure 7:549
44. Ogata H, Mizoguchi Y, Mizuno N, Miki K, Adachi S, Yasuoka N, Yagi T, Yamauchi O, Hirota S, Higuchi Y (2002) J Am Chem Soc 124:11628
45. Montet Y, Amara P, Volbeda A, Vernede X, Hatchikian EC, Field MJ, Frey M, Fontecilla-Camps JC (1997) Nat Struct Biol 4:523
46. Volbeda A, Montet Y, Vernède X, Hatchikian EC, Fontecilla-Camps JC (2002) Int J Hydrogen Energy 27:1449

47. Matias PM, Soares CM, Saraiva LM, Coelho R, Morais J, Le Gall J, Carrondo MA (2001) J Biol Inorg Chem 6:63
48. Frey M, Fontecilla-Camps JC, Volbeda A (2001) Ni,Fe-Hydrogenases. In: Messerschmidt A, Huber R, Poulos T, Wieghardt K (eds) Handbook of Metalloproteins. Wiley, New York, p 880
49. Garcin E, Vernede X, Hatchikian EC, Volbeda A, Frey M, Fontecilla-Camps JC (1999) Structure 7:557
50. Volbeda A, Martin L, Cavazza C, Matho M, Faber BW, Roseboom W, Albracht SP, Garcin E, Rousset M, Fontecilla-Camps JC (2005) J Biol Inorg Chem 10:239
51. Ogata H, Hirota S, Nakahara A, Komori H, Shibata N, Kato T, Kano K, Higuchi Y (2005) Structure 13:1635
52. Bagley KA, Duin EC, Roseboom W, Albracht SPJ, Woodruff WH (1995) Biochemistry 34:5527
53. Happe RP, Roseboom W, Pierik AJ, Albracht SPJ, Bagley KA (1997) Nature 385:126
54. De Lacey AL, Hatchikian EC, Volbeda A, Frey M, Fontecilla-Camps JC, Fernandez VM (1997) J Am Chem Soc 119:7181
55. Pierik AJ, Roseboom W, Happe RP, Bagley KA, Albracht SPJ (1999) J Biol Chem 274:3331
56. Pierik AJ, Hulstein M, Hagen WR, Albracht SPJ (1998) Eur J Biochem 258:572
57. Peters JW, Lanzilotta WN, Lemon BJ, Seefeldt LC (1998) Science 282:1853
58. Nicolet Y, De Lacey AL, Vernède X, Fernandez VM, Hatchikian EC, Fontecilla-Camps JC (2001) J Am Chem Soc 123:1596
59. Lyon EJ, Shima S, Boecher R, Thauer RK, Grevels FW, Bill E, Roseboom W, Albracht SP (2004) J Am Chem Soc 126:14239
60. Brecht M, Van Gastel M, Buhrke T, Friedrich B, Lubitz W (2003) J Am Chem Soc 125:13075
61. Reissmann S, Hochleitner E, Wang H, Paschos A, Lottspeich F, Glass RS, Bock A (2003) Science 299:1067
62. Roseboom W, Blokesch M, Böck A, Albracht SP (2005) FEBS Lett 579:469
63. Vignais PM, Colbeau A (2004) Curr Issues Mol Biol 6:159
64. Albracht SPJ (1994) Biochim Biophys Acta 1188:167
65. Cammack R, Robson R, Frey M (eds) (2001) Hydrogen as a fuel. Learning from Nature. Taylor and Francis, London
66. Maroney MJ, Bryngelson PA (2001) J Biol Inorg Chem 6:453
67. Volbeda A, Fontecilla-Camps JC (2003) Dalton Trans 21:4030
68. Armstrong FA (2004) Curr Opin Chem Biol 8:133
69. Best SP (2005) Coord Chem Rev 249:1536
70. De Lacey AL, Fernandez VM, Rousset M (2005) Coord Chem Rev 249:1596
71. Vignais PM (2005) Coord Chem Rev 249:1677
72. Armstrong FA, Albracht SP (2005) Phil Trans Royal Soc A 363:937
73. Niu S, Thomson LM, Hall MB (1999) J Am Chem Soc 121:4000
74. Amara P, Volbeda A, Fontecilla-Camps JC, Field MJ (1999) J Am Chem Soc 121:4468
75. De Gioia L, Fantucci P, Guigliarelli B, Bertrand P (1999) Inorg Chem 38:2658
76. Siegbahn PEM, Blomberg MRA, Wirstam M, Crabtree RH (2001) J Biol Inorg Chem 6:460
77. Stadler C, De Lacey AL, Montet Y, Volbeda A, Fontecilla-Camps JC, Conesa JC, Fernandez VM (2002) Inorg Chem 41:4424
78. Stein M, Lubitz W (2004) J Inorg Biochem 98:862
79. Liu P, Rodriguez JA (2005) J Am Chem Soc 127:14871

80. Bleijlevens B, Van Broekhuizen FA, De Lacey AL, Roseboom W, Fernandez VM, Albracht SPJ (2004) J Biol Inorg Chem 9:743
81. Happe RP, Roseboom W, Albracht SPJ (1999) Eur J Biochem 259:602
82. De Lacey AL, Stadler C, Fernandez VM, Hatchikian EC, Fan H-J, Li S, Hall MB (2002) J Biol Inorg Chem 7:318
83. Dole F, Medina M, More C, Cammack R, Bertrand P, Guigliarelli B (1996) Biochemistry 35:16399
84. Evans DJ, Pickett CJ (2003) Chem Soc Rev 32:268
85. Artero V, Fontecave M (2005) Coord Chem Rev 249:1518
86. Bouwman E, Reedijk J (2005) Coord Chem Rev 249:1555
87. Dobbek H, Svetlitchnyi V, Gremer L, Huber R, Meyer O (2001) Science 293:1281
88. Dobbek H, Svetlitchnyi V, Liss J, Meyer O (2004) J Am Chem Soc 126:5382
89. Drennan CL, Heo J, Sintchak MD, Schreiter F, Ludden PW (2001) Proc Natl Acad Sci USA 98:11973
90. Doukov TI, Iverson TM, Seravalli J, Ragsdale SW, Drennan CL (2002) Science 298:567
91. Darnault C, Volbeda A, Kim EJ, Legrand P, Vernède X, Lindahl PA, Fontecilla-Camps JC (2003) Nat Struct Biol 10:271
92. Kim EJ, Feng J, Bramlett MR, Lindahl PA (2004) Biochemistry 43:5728
93. Hu Z, Spangler NJ, Anderson ME, Xia JQ, Ludden PW, Lindahl PA, Münck E (1996) J Am Chem Soc 118:830
94. Volbeda A, Fontecilla-Camps JC (2005) Dalton Trans 21:3443
95. Feng J, Lindahl PA (2004) J Am Chem Soc 126:9094
96. Ensign SA (1995) Biochemistry 34:5372
97. Lindahl PA (2002) Biochemistry 41:2097
98. Chen J, Huang S, Seravalli J, Gutzman H Jr, Swartz DJ, Ragsdale SW, Bagley KA (2003) Biochemistry 42:14822
99. Heo J, Staples CR, Halbieb CM, Ludden PW (2000) Biochemistry 39:7956
100. Anderson ME, Lindahl PA (1994) Biochemistry 33:8702
101. DeRose VJ, Telser J, Anderson ME, Lindahl PA, Hoffman BM (1998) J Am Chem Soc 120:8767
102. Seravalli J, Kumar M, Lu WP, Ragsdale SW (1995) Biochemistry 34:7879
103. Anderson ME, Lindahl PA (1996) Biochemistry 35:8371
104. Svetlitchnyi V, Dobbek H, Meyer-Klaucke W, Meins T, Thiele B, Romer P, Huber R, Meyer O (2004) Proc Natl Acad Sci USA 101:446
105. Volbeda A, Fontecilla-Camps JC (2004) J Biol Inorg Chem 9:525
106. Tan X, Loke HK, Fitch S, Lindahl PA (2005) J Am Chem Soc 127:5833
107. Seravalli J, Gu W, Tam A, Strauss E, Begley TP, Cramer SP, Ragsdale SW (2003) Proc Natl Acad Sci USA 100:3689
108. Golden ML, Rampersad MV, Reibenspies JH, Darensbourg MY (2003) Chem Commun (Camb) 7:1824
109. Krishnan R, Voo JK, Riordan CG, Zakharov L, Rheingold AL (2003) J Am Chem Soc 125:4422
110. Linck RC, Spahn CW, Rauchfuss TH, Wilson SR (2003) J Am Chem Soc 125:8700
111. Bramlett MR, Tan X, Lindahl PA (2003) J Am Chem Soc 125:9316
112. Seravalli J, Xiao Y, Gu W, Cramer SP, Antholine WE, Krymov V, Gerfen GJ, Ragsdale SW (2004) Biochemistry 43:3944
113. Gencic S, Grahame DA (2003) J Biol Chem 278:6101
114. Funk T, Gu W, Friedrich S, Wang H, Gencic S, Grahame DA, Cramer SP (2004) J Am Chem Soc 126:88

115. Russell WK, Stålhandske CMV, Xia J, Scott RA, Lindahl PA (1998) J Am Chem Soc 120:7502
116. Tan X, Bramlett MR, Lindahl PA (2004) J Am Chem Soc 126:5954
117. Barondeau DP, Kassmann CJ, Bruns CK, Tainer JA, Getzoff ED (2004) Biochemistry 43:8038
118. Wuerges J, Lee JW, Yim YI, Yim HS, Kang SO, Carugo KD (2004) Proc Natl Acad Sci USA 101:8569
119. Hegg EL (2004) Acc Chem Res 37:775
120. Riordan CG (2004) J Biol Inorg Chem 9:542
121. Evans DJ (2005) Coord Chem Rev 249:1582
122. Harrop TC, Mascharak PK (2005) Coord Chem Rev 249:3007
123. Fan C, Gorst CM, Ragsdale SW, Hoffman BM (1991) Biochemistry 30:431
124. Heo J, Skjeldal L, Staples CR, Ludden PW (2002) J Biol Inorg Chem 7:810
125. Nicolet Y, Lemon BJ, Fontecilla-Camps JC, Peters JW (2000) Trends Biochem Sci 25:138
126. Shima S, Lyon EJ, Thauer RK, Mienert B, Bill E (2005) J Am Chem Soc 43:10430
127. Coremans JMCC, Van Garderen CJ, Albracht SPJ (1992) Biochim Biophys Acta 1119:148
128. Barondeau DP, Roberts LM, Lindahl PA (1994) J Am Chem Soc 116:3442
129. Pershad HR, Duff JL, Heering HA, Duin EC, Albracht SPJ, Armstrong FA (1999) Biochemistry 38:8992
130. Dementin S, Burlat B, De Lacey AL, Pardo A, Adryanczyk-Perrier G, Guigliarelli B, Fernandez VM, Rousset M (2004) J Biol Chem 279:10508
131. Jones AK, Sillery E, Albracht SPJ, Armstrong FA (2002) Chem Commun 866
132. Seravalli J, Kumar M, Lu W-P, Ragsdale SW (1997) Biochemistry 36:11241
133. Gu W, Seravalli J, Ragsdale SW, Cramer SP (2004) Biochemistry 43:9029
134. Menon S, Ragsdale SW (1996) Biochemistry 35:15814
135. Lu ZL, Crabtree RH (1995) J Am Chem Soc 117:3994
136. Forster D (1976) J Am Chem Soc 98:846
137. Seravalli J, Kumar M, Ragsdale SW (2002) Biochemistry 41:1807
138. George SJ, Seravalli J, Ragsdale SW (2005) J Am Chem Soc 127:13500
139. Grahame DA, Khangulov S, DeMoll E (1996) Biochemistry 35:593
140. Barondeau DP, Lindahl PA (1997) J Am Chem Soc 119:3959
141. Tan XS, Sewell C, Yang Q, Lindahl PA (2003) J Am Chem Soc 125:318
142. Lindahl PA (2004) J Biol Inorg Chem 9:516
143. Schenker RP, Brunold TC (2003) J Am Chem Soc 125:13962
144. Amara P, Volbeda A, Fontecilla-Camps JC, Field MJ (2005) J Am Chem Soc 127:2776
145. Maynard EL, Lindahl PA (2001) Biochemistry 40:13262
146. Thauer RK, Jungermann K, Decker K (1977) Bacteriol Rev 41:100
147. Schulte MD, Rogers KL (2004) Geochim Cosmochim Acta 68:1087
148. George SJ, Kurkin S, Thorneley RN, Albracht SPJ (2004) Biochemistry 43:6808